Chinese Journal of Health Management
Volume 20 Issue 3, Year of Publication 2026, Page 273-289 | DoI-10.564220/1674-0815.2026.054

ISSN: 1674-0815

cjhmonline.com

DoI-10.564220/1674-0815

Chinese Journal of Health Management

Chinese Medical Association

Comparative QBD guided optimization of spray-drying versus hot-melt extrusion for Alectinib ASD

Abhishek Jain[1], Pragna Shelat[2]
[1]Research scholar Kadi sarva Vishwavidhyalaya (KSV), Gandhinagar, Gujarat.
[2]Professor, Dept. Pharmaceutics KB Raval College of Pharmacy, Ahmedabad, Gujarat.
Corresponding Author Email id: **rxjainabhi@gmail.com**

Article Information
Received: 17-10-2025
Revised: 22-11-2025
Accepted: 17-01-2026
Published: 15-03-2026

Keywords:
Alectinib hydrochloride, amorphous solid dispersion, Quality by Design, spray drying, hot-melt extrusion, Soluplus

ABSTRACT:

Background: Alectinib hydrochloride exhibits severe aqueous solubility limitations (0.022 mg/mL) that compromise therapeutic efficacy. This study employed Quality-by-Design principles to systematically compare spray-drying and hot-melt extrusion platforms for amorphous solid dispersion development. **Methods:** D-optimal experimental designs optimized critical formulation parameters across both platforms. Spray-drying utilized Central Composite Design (18 runs) while hot-melt extrusion employed extreme-vertices design (16 runs). Drug loading was maintained at 40% w/w with Soluplus®/Vitamin E TPGS optimization. Comprehensive characterization included equilibrium solubility, USP dissolution, solid-state analysis, and ICH-compliant stability assessment. **Results:** Both platforms achieved complete amorphization with exceptional model performance (R^2 > 95%). Compared to crystalline drug, spray-dried dispersions improved solubility by over 11-fold (≈256 µg/mL) and reached ~95% release at 45 min. HME formulations showed a slightly higher solubility (~269 µg/mL) with ~94% dissolution under identical conditions. Accelerated stability Under 40 °C/75% RH, spray-dried dispersions retained ~97% of initial performance after 6 months versus ~89% for HME, suggesting approximate shelf lives of 22 and 17 months, respectively. **Conclusion:** Both platforms successfully address alectinib's biopharmaceutical challenges while offering distinct advantages. Spray-drying provides superior long-term stability for premium applications, whereas hot-melt extrusion delivers enhanced manufacturing efficiency with four-fold higher throughput and solvent-free processing for large-scale production.

ABBREVIATIONS

ASD, Amorphous solid dispersion; BBD, Box–Behnken design; BCS, Biopharmaceutics Classification System; CCD, Central Composite Design; CQAs, Critical Quality Attributes; DE_{45}, Dissolution efficiency at 45 minutes; DMSO, Dimethyl sulfoxide; DSC, Differential scanning calorimetry; D-optimal, D-optimal design; FMEA, Failure Mode and Effects Analysis; FTIR, Fourier transform infrared spectroscopy; HME, Hot-melt extrusion; ICH, International Council for Harmonisation; LA-HME, Liquid-assisted hot-melt extrusion; PAT, Process

Chinese Journal of Health Management
Volume 20 Issue 3, Year of Publication 2026, Page 273-289 | DoI-10.564220/1674-0815.2026.054

Analytical Technology; PXRD, Powder X-ray diffraction; QbD, Quality-by-Design; QTPP, Quality Target Product Profile; RPN, Risk Priority Number; SD, Spray d rying; SLS, Sodium lauryl sulfate; TPGS, D-α-tocopherol polyethylene glycol 1000 succinate (Vitamin E TPGS); USP, United States Pharmacopeia.

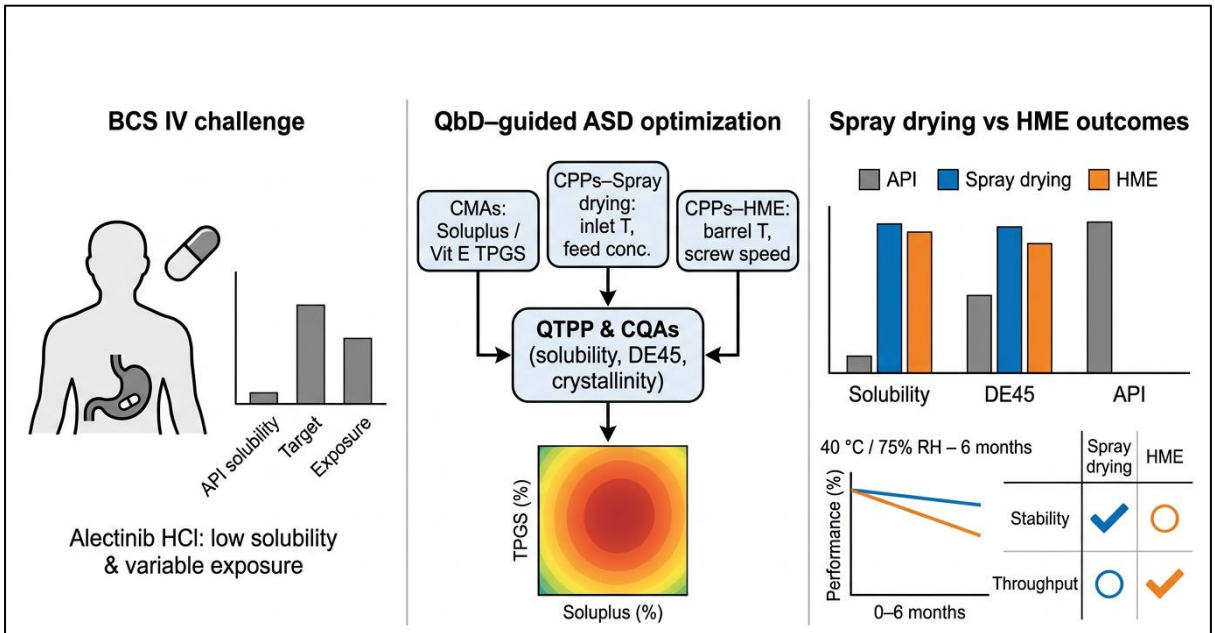

QbD-enabled comparison of spray drying and hot-melt extrusion guides platform selection for alectinib amorphous solid dispersions.

1. INTRODUCTION:

Many new molecular entities struggle with poor water solubility—affecting more than two-thirds of candidates—and this is especially problematic for BCS Class IV drugs that exhibit both limited dissolution and permeability[1,2,3,4], creating substantial barriers to achieving therapeutic level[5,6]. Contemporary development strategies must simultaneously address immediate dissolution enhancement, long-term physical stability, manufacturing scalability, and regulatory compliance requirements[7,8].

As a next-generation ALK inhibitor, alectinib hydrochloride has demonstrated enhanced antitumor activity compared to first-line agents, yet it remains hampered by very low aqueous solubility (0.022 mg/mL) across physiological pH conditions[9,10], classified as practically insoluble according to pharmacopeial standards[11,12]. Existing commercial products achieve only 37% oral bioavailability under fed conditions[13], with pronounced food effects (2.9-fold enhancement) indicating dissolution-limited absorption characteristics[14,15]. Inter-patient pharmacokinetic variability exceeds 40%, reflecting inconsistent gastrointestinal dissolution processes that compromise therapeutic predictability[3]. These biopharmaceutical constraints require elevated dosing with associated toxicity risks, emphasizing the need for advanced formulation approaches.

Formulating drugs as amorphous solid dispersions disrupts their crystalline lattice and disperses molecules within a polymer matrix, thereby markedly improving dissolution rates[16,17]. This approach stabilizes drug molecules via molecular integration within polymeric matrices, eliminating crystal lattice energy barriers while enhancing dissolution thermodynamics[4,18]. Enhancement mechanisms include expanded surface area, improved wetting characteristics, and drug-polymer molecular complex formation[19,20]. The amorphous state's elevated Gibbs free energy provides thermodynamic driving force for enhanced dissolution, while polymeric carriers supply kinetic stabilization against rapid recrystallization[21,22]. Regulatory acceptance has grown substantially, with ASD-based products representing 68% of recent BCS Class II/IV approvals[23,24,45,46].

Technology selection requires comprehensive evaluation of technical performance, economic considerations, and regulatory implications. Spray drying operates through rapid solvent evaporation from atomized droplets, enabling precise particle formation with minimal thermal exposure[25,26,27,28]. Hot-melt extrusion provides continuous, solvent-free processing through combined thermal and mechanical energy input, creating intimate molecular

mixing with superior throughput capabilities[29,30,31,32]. Each platform offers distinct advantages: spray drying delivers exceptional flexibility for thermolabile compounds through low-temperature operation, while hot-melt extrusion enables continuous manufacturing with environmental benefits through solvent elimination. Platform-specific limitations include solvent management complexity versus thermal stress considerations respectively[33,34].

Quality-by-Design (QbD) principles were employed to establish a robust design space by defining critical material attributes and process parameters[35,36,37,38], while risk assessment and ICH Q8(R2)–guided QTPP development ensured objective, regulation-aligned platform comparison for spray-drying versus hot-melt extrusion[39,40,41,42,43,44].

In addition to comprehensive characterization of immediate performance attributes, this study incorporated rigorous accelerated stability testing under ICH-recommended conditions (40°C/75% RH) enabling direct assessment of how each processing method affected long-term product integrity[76,77]. The results revealed clear platform-dependent differences: spray-dried amorphous dispersions consistently maintained superior retention of solubility and dissolution efficiency over six months, and exhibited a much lower rise in residual crystallinity compared to hot-melt extruded counterparts. These findings highlight that reduced thermal exposure during spray drying preserves the amorphous structure more effectively, while the extended heat input in hot-melt extrusion can foster increased molecular mobility and recrystallization upon storage. By integrating these stability outcomes with other performance parameters, the evaluation demonstrates that optimized spray drying offers a distinct advantage for products requiring maximal shelf-life and robustness, whereas hot-melt extrusion provides compelling benefits in terms of scalability and solvent-free manufacturing. Ultimately, this systematic, QbD-guided comparison not only delivers the first in-depth, stability-focused platform selection framework for alectinib, but also establishes broadly applicable criteria for rational technology choice in BCS Class IV drug development.

2. MATERIALS AND METHODS:

2.1 Materials:

Alectinib hydrochloride (≥99.5% purity) was obtained as a gift sample from Cadila Healthcare Limited (Ahmedabad, India). Soluplus® (polyvinyl caprolactam-polyvinyl acetate-polyethylene glycol graft copolymer) was supplied by BASF Corporation (Ludwigshafen, Germany)[77]. Vitamin E TPGS (D-α-tocopherol polyethylene glycol 1000 succinate) was purchased from Isochem (Paris, France)[47]. mannitol from Roquette and Sodium lauryl sulfate (SLS), dimethyl sulfoxide (DMSO), and analytical-grade solvents were obtained from Sigma-Aldrich (St. Louis, MO, USA)[49]. were used. All solvents were HPLC-grade (Fisher Scientific)[50]. Excipients for formulation included croscarmellose sodium (JRS Pharma), colloidal silicon dioxide (Evonik), and magnesium stearate (Peter Greven) and capsule (ACG). All excipients met current USP-NF specifications with certificates of analysis confirming identity and purity[50].

HPLC-grade acetonitrile (≥99.9%) and methanol (≥99.8%) were supplied by Fisher Scientific (Hampton, NH, USA)[50]. Phosphoric acid (85%, ACS grade) was obtained from Merck KGaA (Darmstadt, Germany)[51]. Dichloromethane (≥99.5%) and ethanol (≥99.8%) for spray drying met ICH Q3C(R6) residual solvent specifications [52]. Purified water was generated using Milli-Q Advantage A10 system (Millipore, Burlington, MA, USA) with conductivity <1.3 µS/cm [53].

2.2 Equipment and Instrumentation:

Spray drying was performed on a Büchi B-290 Mini Spray Dryer fitted with a closed-loop N_2 system and 7 µm mesh atomizer, under parameters specified by the manufacturer and integrated monitoring was used for spray drying operations [54]. Hot-melt extrusion employed a Thermo Scientific Pharma-16 twin-screw extruder (Thermo Fisher Scientific, Karlsruhe, Germany) with co-rotating intermeshing screws (L/D ratio 25:1) and six independently controlled heating zones [55].

Analytical characterization utilized an Agilent 1260 Infinity II LC System with Phenomenex Luna C18 column (250 × 4.6 mm, 5 µm) [56], Electrolab EDT-08L dissolution apparatus with USP Apparatus II configuration [57], Bruker D8 Advance X-ray diffractometer with Cu Kα radiation, TA Instruments Q2000 differential scanning calorimeter with nitrogen purge, and PerkinElmer Spectrum Two FTIR spectrometer with ATR accessory [58].

2.3 Physicochemical Characterization:

Equilibrium solubility was determined across physiological pH ranges (1.2, 4.5, 6.8, 7.4) using standardized

shake-flask methodology.[59] Excess drug (50 mg) was equilibrated in 10 mL medium at 37.0 ± 0.5°C for 24 hours with orbital shaking (100 rpm), centrifuged (10,000 rpm, 10 minutes), filtered (0.45 µm PTFE), and analyzed by validated HPLC within 30 minutes [60]. Thermal characterization employed DSC analysis of 3-5 mg samples in sealed aluminum pans using 10°C/min heating from -20°C to 350°C under nitrogen, with glass transitions determined by midpoint methodology [61]. Powder properties were evaluated according to USP <616> methods, with particle size distribution measured by laser diffraction (Malvern Mastersizer 3000) using dry dispersion [62].

2.4 Quality-by-Design Framework Implementation:

A systematic ICH Q8(R2)-compliant approach guided comparative platform evaluation through structured risk assessment and statistical optimization [64,65]. The framework encompassed Quality Target Product Profile (QTPP) definition, failure mode and effects analysis (FMEA)-based risk assessment, identification of Critical Quality Attributes (CQAs), Critical Material Attributes (CMAs), and Critical Process Parameters (CPPs), followed by design space characterization via D-optimal experimental designs tailored to each platform's operational constraints.

Critical Attributes identified were Equilibrium solubility (≥220 µg/mL representing 10-fold enhancement target), dissolution efficiency at 45 minutes (≥90% for bioavailability assurance), and residual crystallinity (<5% for physical stability maintenance).

Experimental Design Strategy: Spray-drying optimization utilized Central Composite Design CCD with $\alpha = 2.0$, initially generating 30 design points. A D-optimal algorithm then selected 18 experiments to maximize estimation precision within two balanced blocks [68], investigating polymer ratios (Soluplus® 70-90%, TPGS 10-30%), thermal parameters (inlet temperature 100-120°C), and feed characteristics (concentration 5-15% w/v) [66]. Hot-melt extrusion employed Extreme Vertices Design (generating 20 candidate points within the constrained mixture space, with D-optimal selection identifying 16 runs optimized for mixture-process parameter estimation while maintaining practical manufacturing constraints (barrel temperature 180-220°C, screw speed 80-120 rpm) [67,69].

2.5 Analytical Methods and Validation:

Chromatographic Analysis:

Quantitative analysis employed validated stability-indicating HPLC methodology using Waters ACQUITY UPLC system with photodiode array detection at 278 nm. Chromatographic separation utilized Phenomenex Luna C18 column (4.6×150 mm, 5 µm particle size) with mobile phase comprising acetonitrile:phosphate buffer (60:40 v/v, pH 3.0), flow rate 1.0 mL/min, injection volume 20 µL, and 8-minute runtime. Method validation parameters satisfied ICH Q2(R1) requirements: linearity coefficient r^2 >0.999 across 5-50 µg/mL range, precision with relative standard deviation <2.0%, accuracy demonstrating 98.0-102.0% recovery, and specificity confirmed against potential degradation products [63].

Physicochemical Characterization:

Equilibrium solubility assessment utilized standardized shake-flask methodology across physiological pH conditions (buffers at pH 1.2, 4.5, 6.8, and 7.4). Excess sample (50 mg) equilibrated in 10 mL buffer medium at 37.0±0.5°C for 24 hours under orbital agitation (100 rpm), followed by centrifugation (10,000 rpm, 10 minutes), filtration through 0.45 µm PTFE membrane, and immediate HPLC quantification.

Thermal characterization employed differential scanning calorimetry (DSC 3+, Mettler Toledo) analyzing 3-5 mg samples in sealed aluminum pans with 10°C/min heating rate from -20°C to 350°C under nitrogen atmosphere [61]. Crystallinity evaluation utilized X-ray powder diffraction (Bruker D8 Advance) with Cu Kα radiation, scanning 2θ range 5-60° at 0.02° step size and 1 second count time [73,74]. Molecular interaction assessment employed Fourier-transform infrared spectroscopy (Bruker Alpha FTIR) in attenuated total reflectance mode across 4000-400 cm^{-1} range with 32 scans at 4 cm^{-1} resolution [75].

2.6 Manufacturing Protocols:

Spray drying protocol involved solution preparation where drug and polymeric excipients were accurately weighed and dissolved in dichloromethane:methanol (1:1 v/v) to achieve target concentrations, with solutions

magnetically stirred for 2 hours, filtered through 0.45 µm PTFE membrane, and processed according to design parameters [70]. Processing parameters included variable inlet temperature (100-120°C), monitored outlet temperature (62-65°C), controlled feed rate (5.0 mL/min by peristaltic pump), piezoelectric mesh atomization (7.0 µm aperture), nitrogen drying gas flow (120 L/h closed-loop system), and maximum aspirator setting (100% suction). Post-processing involved vacuum-drying collected powder at 25°C for 48 hours (confirmed by Karl Fischer titration, target <0.5%), followed by storage in amber containers with desiccant at 2-8°C [70,80].

Hot-melt extrusion protocol began with material preparation where drug and polymeric components were pre-blended using V-blender for 15 minutes at 25 rpm, with blend uniformity verified by HPLC analysis (RSD <2%). Processing parameters included variable temperature profile (180-220°C barrel temperature), variable screw speed (80-120 rpm), controlled feed rate (1.0 kg/h gravimetric feeding), calculated residence time (90-120 seconds from tracer studies), and screw configuration comprising conveying elements (feed zone), kneading blocks (melting/mixing), and distributive mixing elements. Post-processing involved immediate cooling of extruded strands on chilled conveyor belt, milling to <250 µm, and storage in sealed containers with desiccant [71].

2.7 Stability Studies:

Accelerated stability studies were conducted according to ICH Q1A(R2) guidelines at 40°C/75% RH [76]. Sampling schedule included initial, 1, 2, 3, and 6 months with comprehensive analytical assessment including chemical stability (HPLC), physical stability (PXRD, DSC), and performance stability (dissolution) [45].

2.8 Statistical Analysis Protocols:

All statistical analyses employed Minitab Statistical Software version 19.2020.1 (Minitab Inc., State College, PA, USA) with significance level $\alpha = 0.05$. Response surface methodology utilized D-optimal experimental designs with model validation criteria: $R^2 > 0.85$, adjusted R^2 within 0.20 of R^2, predicted $R^2 > 0.70$, adequate precision >4.0, and lack-of-fit p-value >0.05.

Model Selection: Hierarchical model building prioritized significant terms ($p < 0.05$) while maintaining model hierarchy. ANOVA F-tests assessed overall model significance, with post-hoc pairwise comparisons using Tukey's HSD test. Bonferroni correction applied for multiple endpoint analyses.

Optimization: Multi-response optimization employed desirability function approach, with numerical optimization seeking composite desirability ≥0.80. Design space definition utilized prediction intervals with 95% confidence level for robust operating ranges.

3. RESULTS AND DISCUSSION:

3.1 Physicochemical Properties and Initial Formulation Assessment:

Alectinib hydrochloride manifested typical challenges associated with BCS Class IV compounds, necessitating sophisticated formulation strategies to overcome inherent bioavailability limitations [18,20]. Preliminary evaluation revealed the raw drug powder possesses poor compressibility (Carr's Index 35.3 ± 1.2%; Hausner Ratio 1.55 ± 0.08), indicating a propensity for flow issues during manufacturing. Aqueous solubility assessment demonstrated extremely limited dissolution across physiological pH ranges, with maximum solubility of only 22.1 ± 1.2 µg/mL observed in pH 1.2 buffer medium. This negligible aqueous solubility, combined with moderate permeability characteristics, confirmed the BCS Class IV classification and highlighted the critical need for solubility enhancement strategies.

Thermal characterization using differential scanning calorimetry revealed a high decomposition temperature exceeding 300°C, with substantial fusion enthalpy of 95.6 ± 2.1 J/g, indicating robust intermolecular crystalline interactions requiring significant thermodynamic energy for disruption during amorphous conversion processes. Laser diffraction particle sizing indicated a D_{50} of 0.141 ± 0.018 µm; however, poor wetting limited the dissolution benefits of this fine particle size, underscoring the need for amorphous dispersion strategies.

pH solubility profiling demonstrated negligible variation (20.6 ± 1.2 to 22.1 ± 1.6 µg/mL) across pH 1.2–9.0 (ANOVA $F = 2.14$, $p = 0.156$), confirming that simple pH adjustment would not appreciably increase solubility. Consequently, rapid screening of solid dispersions via kneading was conducted using combinations of Soluplus® and Vitamin E TPGS. One-way ANOVA highlighted significant differences among seven excipient systems ($F =$

156.7, $p < 0.001$) [82]. Tukey's HSD test identified the Soluplus®/TPGS blend (1:0.5:0.5 drug:TPGS:Soluplus®) as the most effective, elevating solubility to 0.160 ± 0.014 mg/mL an eightfold increase over crystalline API and demonstrating robust physical stability.

Table 1: Solubility Enhancement Profile of Kneaded Solid Dispersions (n=3, mean ± SD)

Trial	Formulation	Ratio	Solubility (mg/mL)	Enhancement Factor	Statistical Significance*
1	Pure API	-	0.020 ± 0.002	1.0	Reference
2	API + SLS	1:0.5	0.120 ± 0.018	6.0	$p < 0.001$
3	API + Soluplus®	1:1	0.140 ± 0.012	7.0	$p < 0.001$
4	API + Vit. E TPGS	1:0.5	0.130 ± 0.015	6.5	$p < 0.001$
5	API + SLS + Soluplus®	1:0.5:0.5	0.100 ± 0.008	5.0	$p < 0.01$
6	API + SLS + Vit. E TPGS	1:0.5:0.5	0.110 ± 0.009	5.5	$p < 0.01$
7	API + Vit. E TPGS + Soluplus®	1:0.5:0.5	0.160 ± 0.014	8.0	$p < 0.001$

**Compared to pure API using Tukey's post-hoc test*

Subsequent dissolution testing in simulated gastric fluid (pH 1.2) provided further evidence of performance enhancement. The optimized kneaded dispersion released 18.0 ± 2.0% of drug within 10 minutes and reached 68.0 ± 4.0% release at 45 minutes, compared to 6.4 ± 3.0% and 24.0 ± 3.0%, respectively, for the unformulated API. Dissolution efficiency at 45 minutes (DE_{45}) increased from 12.8 ± 2.7% to 38.5 ± 4.8%, indicating not only a faster initial release but also sustained supersaturation over the 90-minute period (87.0 ± 3.8% cumulative release). These findings confirm the synergistic action of Soluplus® (polymeric stabilization) and TPGS (surfactant-mediated wetting) and justify their selection for further evaluation via spray-drying and hot-melt extrusion under Quality-by-Design guidance.

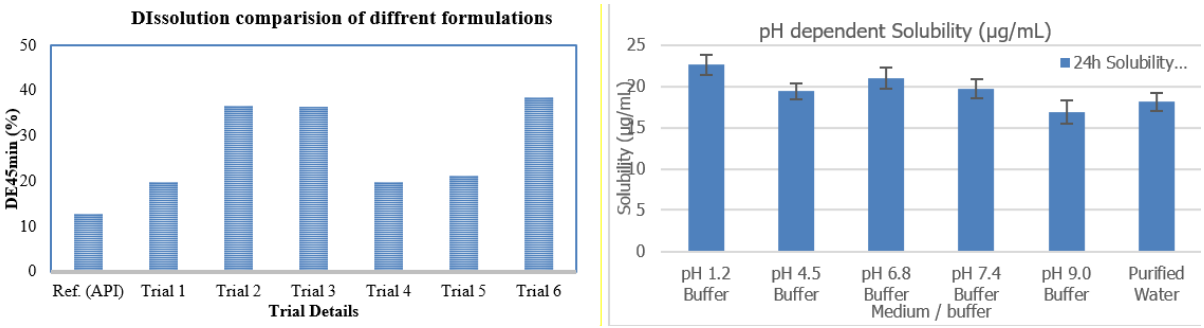

Figure 1: Line graph of pH dependent solubility and dissolution Efficiency at 45 minutes (DE_{45}) for all formulations.

3.2 Experimental Design Outcomes and Statistical Model Performance:

D-optimal experimental designs generated robust regression models meeting pharmaceutical validation standards across both platforms. Spray-drying achieved superior model statistics (solubility R^2 = 99.35%, dissolution R^2 = 99.46%) compared to hot-melt extrusion (R^2 = 96.80% and 95.20%, respectively), with all models demonstrating adequate precision >16.0 and non-significant lack-of-fit ($p > 0.05$).

Spray Drying Experimental outcomes and Response Surface Modelling:

Experimental Matrix and Outcomes:

Central Composite Design encompassed 18 runs investigating Soluplus® (70-90%), TPGS (10-30%), inlet temperature (100-120°C), and feed concentration (5-15% w/v). Solubility responses ranged 198.3-255.6 µg/mL, while dissolution spanned 74.3-95.3%.

Chinese Journal of Health Management
Volume 20 Issue 3, Year of Publication 2026, Page 273-289 | DoI-10.564220/1674-0815.2026.054

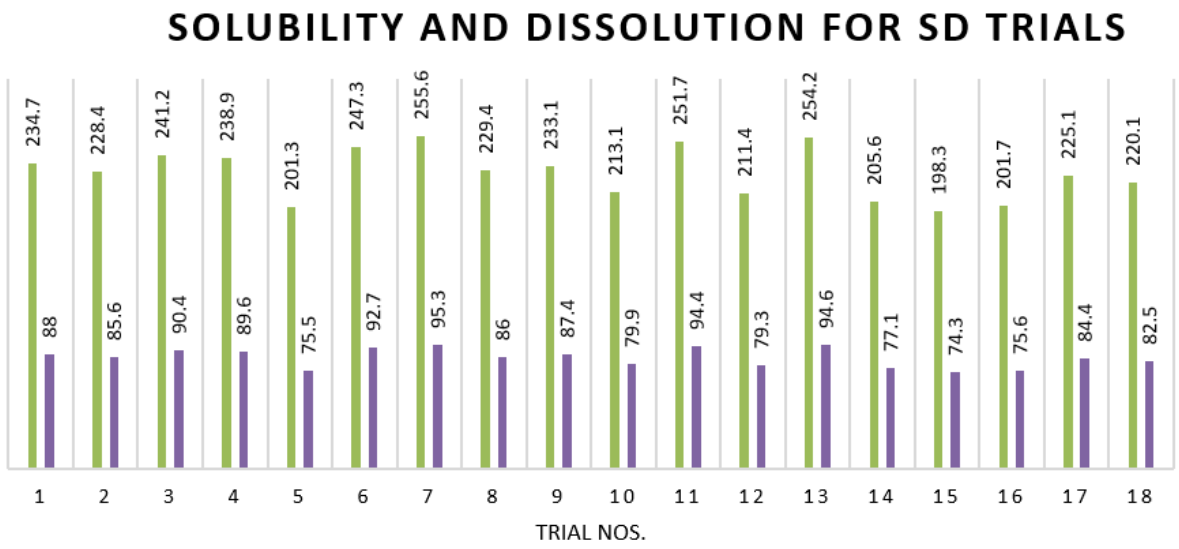

Figure 2: Solubility (µg/ml) and Dissolution (% Dissolved at 45 min) comparison of different Spray Drying (SD) formulation

Model Performance and Factor Significance:

Quadratic regression models achieved exceptional fit metrics: solubility (R^2 = 99.35%, predicted R^2 = 88.50%, AP = 18.6) and dissolution (R^2 = 99.46%, predicted R^2 = 90.70%, AP = 21.4). Soluplus® emerged as the dominant factor for both responses ($p \leq 0.015$), with TPGS providing secondary enhancement ($p \leq 0.048$). Process parameters showed minimal impact within tested ranges, with additive rather than interactive effects governing performance.

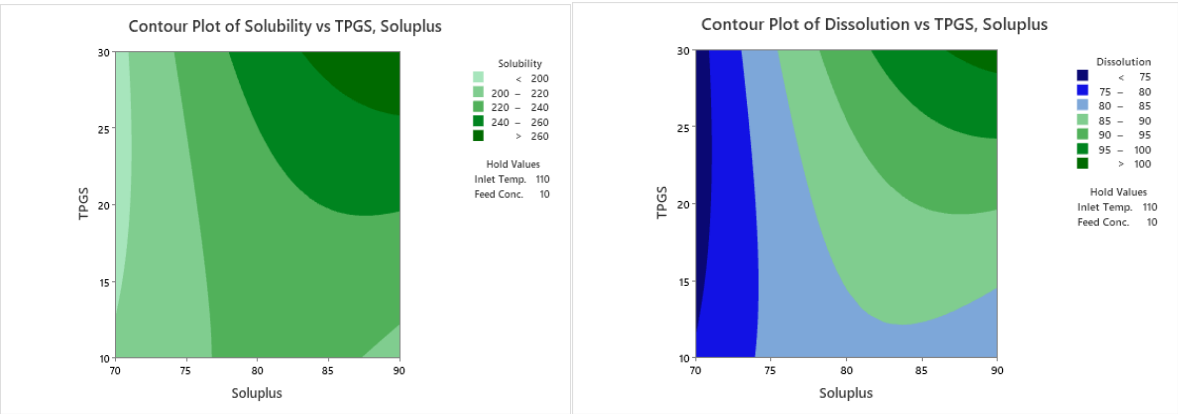

Figure 3 ***Contour plot for Response-Solubility and dissolution***

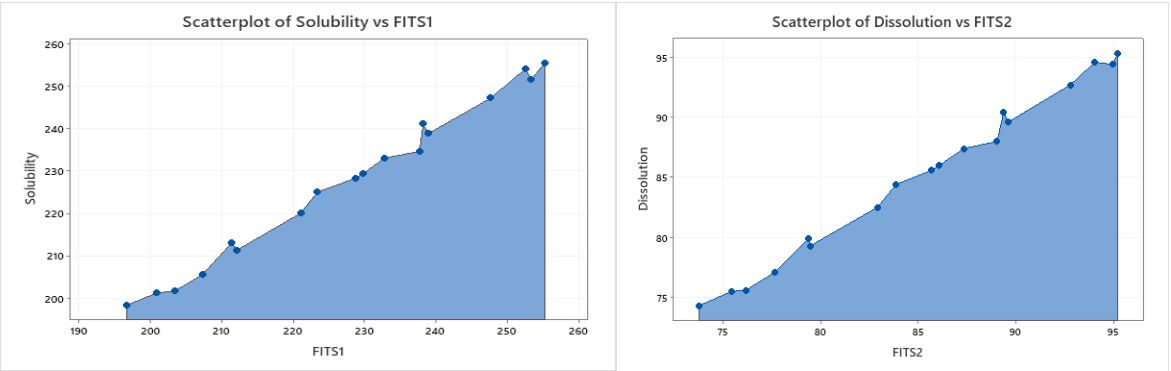

Figure 4 Overlay of predicted vs. observed solubility and dissolution

3.2.2 Hot-Melt Extrusion Experimental outcomes and Mixture-Process Modelling

Design Implementation and Response Range

Extreme vertices design (16 runs) evaluated Soluplus® (75-90%), TPGS (10-25%), barrel temperature (180-220°C), and screw speed (80-120 rpm). Responses demonstrated narrower ranges: solubility 238.9-268.7 µg/mL, dissolution 87.8-93.8%.

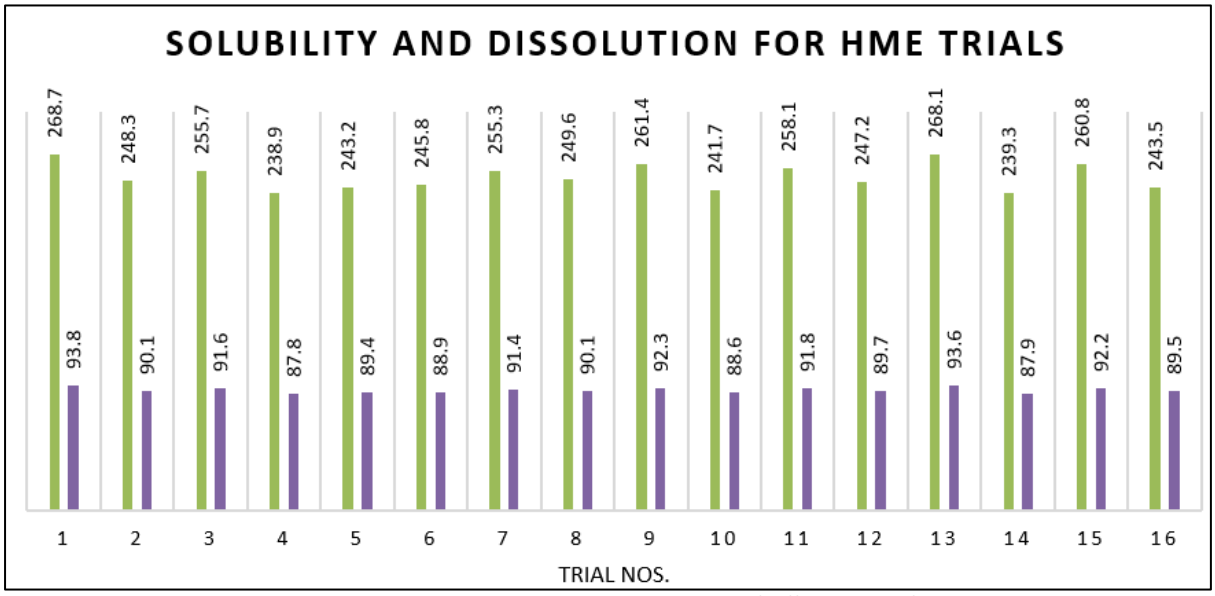

Figure 5: Solubility (µg/ml) and Dissolution (% Dissolved at 45 min) comparison of different HME formulation

Statistical Modelling and Mechanistic Insights:

Mixture-process regression revealed complex interaction patterns. Solubility modeling (R^2 = 96.80%, predicted R^2 = 85.40%, AP = 16.9) identified Soluplus®-TPGS synergism (t = 4.37, p = 0.003) contributing >600 µg/mL enhancement, while screw speed interactions significantly modulated outcomes. Dissolution modeling (R^2 = 95.20%, predicted R^2 = 82.90%, AP = 19.2) confirmed composition dominance over process variables, with Soluplus® showing primary influence (F = 98.24, p <0.05) [84].

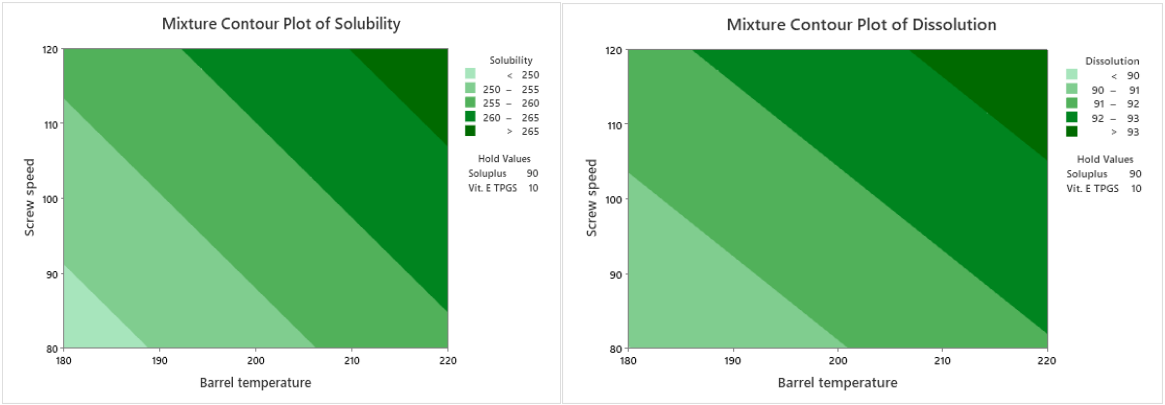

Figure 6 Contour plot for Response-Solubility and Dissolution

3.2.3 Platform Comparison and Optimization:

Both platforms satisfied validation criteria (predicted R^2 >82%, AP >16), though spray-drying demonstrated superior predictive reliability. Multi-response optimization using Derringer-Suich methodology achieved maximum desirability (1.000) for both platforms, with predicted responses closely matching experimental validation (deviations <±2%). Spray-drying's higher determination coefficients suggest more predictable formulation-performance relationships, while HME's mixture-process interactions offer greater mechanistic complexity for targeted optimization strategies.[84,85,86].

3.2.3.2 Multi-Response Optimization:

Simultaneous optimization of solubility and dissolution efficiency at 45 minutes (DE_{45}) was performed using a Derringer–Suich desirability function. Both platforms reached a composite desirability score of 1.000, identifying optimal formulation and process conditions well within the experimental design space. The optimal spray-dried formulation used Soluplus® at 90% w/w and vitamin E TPGS at 30% w/w, processed at an inlet temperature of 100°C with a feed concentration of 13.8% w/v. For HME, the optimal was Soluplus® 87.5%, TPGS 12.5%, at 220°C and 120 rpm. Predicted equilibrium solubility and dissolution approached 303.1 µg/mL and 100% for spray drying, and 275.3 µg/mL and 94.8% for HME, respectively. Observed responses closely matched these predictions, with deviations under ±2%.

3.2.3.3 Experimental Validation:

Model-predicted optimal conditions were experimentally verified with batches from each platform. The observed solubility and DE_{45} values deviated by less than ±2% from model predictions, confirming model robustness and scalability to commercial production settings [87].

3.2.4 Design Space Characterization and Process Insights:

Comparative evaluation of both platforms revealed HME offered higher throughput (2.5 ± 0.2 kg/h vs. 1.2 ± 0.1 kg/h) and superior material recovery ($94.8 \pm 1.7\%$ vs. $87.2 \pm 2.1\%$), supporting process efficiency for commercial-scale production. HME's continuous, solvent-free operation also reduced operational complexity and energy requirements compared to the solvent-based, high-energy spray-drying process [88]. However, thermal stress profiling revealed differences in drug exposure. Spray drying employed rapid evaporation (~5 seconds at 100–112°C), while HME involved extended heating (~105 ± 8 seconds at 220°C), potentially impacting long-term stability [88].

Table: Manufacturing Performance Comparison

Parameter	Spray Drying	Hot-Melt Extrusion	Statistical Significance
Processing Time (min/kg)	180 ± 15	45 ± 5	$p < 0.001^a$
Collection/Yield Efficiency (%)	87.2 ± 2.1	94.8 ± 1.7	$p < 0.001^a$
Energy Consumption (kWh/kg)	3.5 ± 0.3	2.2 ± 0.2	$p < 0.001^a$
Throughput (kg/h)	1.2 ± 0.1	2.5 ± 0.2	$p < 0.001^a$
Solvent Usage (L/kg product)	8.5 ± 0.5	0.0	-
Temperature Exposure Time	<5 seconds	105 ± 8 seconds	-
Process Complexity Score*	8.2 ± 0.4	6.1 ± 0.3	$p < 0.001^a$
Processing Time (min/kg)	180 ± 15	45 ± 5	$p < 0.001^a$

[a] *Unpaired t-test comparison between platforms*

**Complexity score based on number of controlled variables and operational requirements (1-10 scale)*

3.3 Product Performance and Quality Evaluation:

Both ASD approaches yielded statistically equivalent solubility enhancements. Spray-dried ASDs achieved 255.6 ± 10.3 µg/mL (11.6-fold increase), while HME yielded 268.7 ± 10.8 µg/mL (12.2-fold increase), with no significant difference ($p = 0.234$) [89]. One-way ANOVA confirmed superior performance compared to crystalline API ($F = 1247.6$, $p < 0.001$) [89].

Dissolution profiles showed 95.3 ± 1.5% (DE_{45} = 74.62 ± 0.81%) for spray drying and 93.8 ± 1.5% (DE_{45} = 71.49 ± 0.96%) for HME, far exceeding crystalline API (23.4 ± 3.1%; DE_{45} = 14.29 ± 0.78%). ANOVA confirmed significance vs. crystalline API ($F = 2834.6$, $p < 0.001$), with no inter-platform difference ($p = 0.156$) [90].

Chinese Journal of Health Management
Volume 20 Issue 3, Year of Publication 2026, Page 273-289 | DoI-10.564220/1674-0815.2026.054

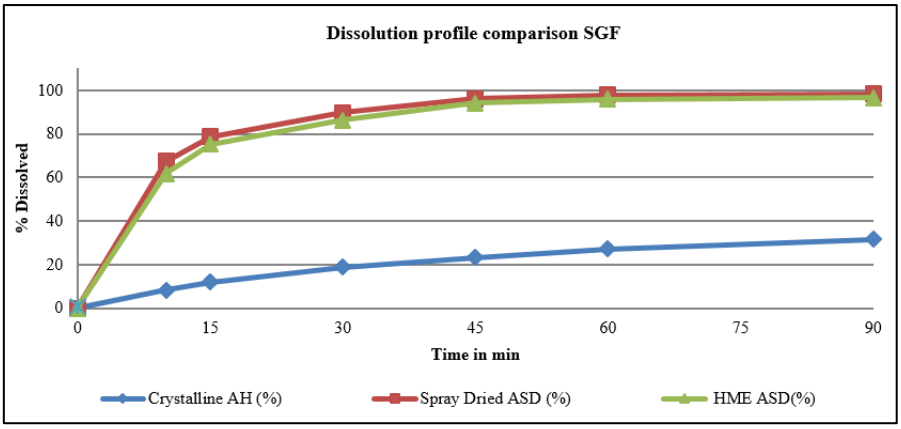

Figure 7: Overlay dissolution profiles for crystalline drug, HME ASD, and spray-dried ASD. in SGF Containing 2.0% Triton

Similarity factor (f_2) analysis comparing ASD platforms to crystalline drug yielded values of 28.43 and 29.57 for spray-dried and hot-melt extruded formulations respectively [94,95], confirming dissimilar dissolution profiles that indicate successful enhancement potential. Platform comparison yielded $f_2 = 67.8$, approaching the similarity threshold and confirming comparable dissolution characteristics between manufacturing approaches despite different processing mechanisms.

3.4 Solid-State Characterization and Molecular Interactions:

Comprehensive solid-state characterization confirmed complete amorphization for both manufacturing platforms while revealing distinct molecular interaction profiles reflecting different processing histories. DSC analysis confirmed complete amorphization, with disappearance of the drug melting peak (301.2°C) and appearance of single glass transition events [96,97]: 86.4 ± 1.2°C (spray drying) and 88.1 ± 1.5°C (HME). These glass transition temperatures, falling intermediate between pure drug and polymer components, confirmed successful molecular-level mixing and drug-polymer miscibility achievement through both processing approaches.

Table: Comprehensive Thermal Analysis Summary

Sample	Melting Point (°C)	Enthalpy (J/g)	Glass Transition (°C)	ΔCp (J/g·K)	Interpretation
Crystalline API - a	301.2 ± 0.8	95.6 ± 2.1	Not observed	-	Fully crystalline
Soluplus® - b	Not observed	-	70.2 ± 1.1	0.34 ± 0.02	Amorphous polymer
Spray Dried ASD - c	Not observed	-	86.4 ± 1.2	0.42 ± 0.03	Fully amorphous
HME ASD -d	Not observed	-	88.1 ± 1.5	0.45 ± 0.03	Fully amorphous

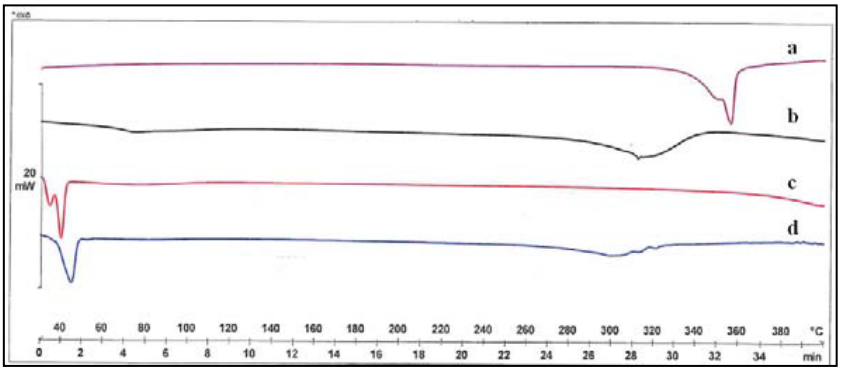

Figure 8: DSC Thermogram of (a) Alectinib hydrochloride (b) Soluplus (c) HME and (d) spray-dried ASDs

3.5.2 X-ray Powder Diffraction Analysis (XRPD):

XRD patterns lacked the sharp reflections of the crystalline drug (e.g., 8.4°, 12.0°, 14.1°, 16.8°, 19.7°, 21.3°, 23.6°, and 25.2° 2θ [98,99], and instead exhibited broad halos near ~20° 2θ that consistent with complete amorphization. Both ASD formulations exhibited broad amorphous halos centered around 20° 2θ, confirming successful conversion to the amorphous state with molecular-level drug dispersion. Rietveld analysis quantified >98% amorphous content for both platforms, with residual crystallinity <1%, validating complete crystalline

lattice disruption [91,92,100,101].

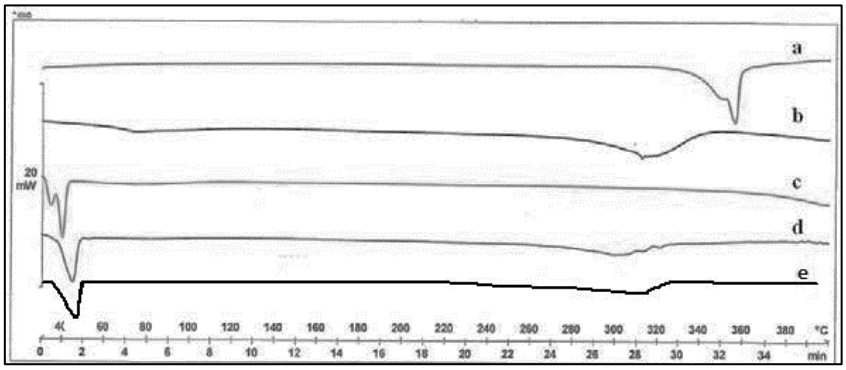

Figure 9: DSC Thermogram of (a) Alectinib hydrochloride (b) Soluplus (c) Vit. E TPGS (d) HME and (e) spray-dried ASDs

3.5.2 X-ray Powder Diffraction Analysis (XRPD):

XRD patterns lacked the sharp reflections of the crystalline drug (e.g., 8.4°, 12.0°, 14.1°, 16.8°, 19.7°, 21.3°, 23.6°, and 25.2° 2θ [98,99], and instead exhibited broad halos near ~20° 2θ that consistent with complete amorphization. Both ASD formulations exhibited broad amorphous halos centered around 20° 2θ, confirming successful conversion to the amorphous state with molecular-level drug dispersion. Rietveld analysis quantified >98% amorphous content for both platforms, with residual crystallinity <1%, validating complete crystalline lattice disruption [91,92,100,101].

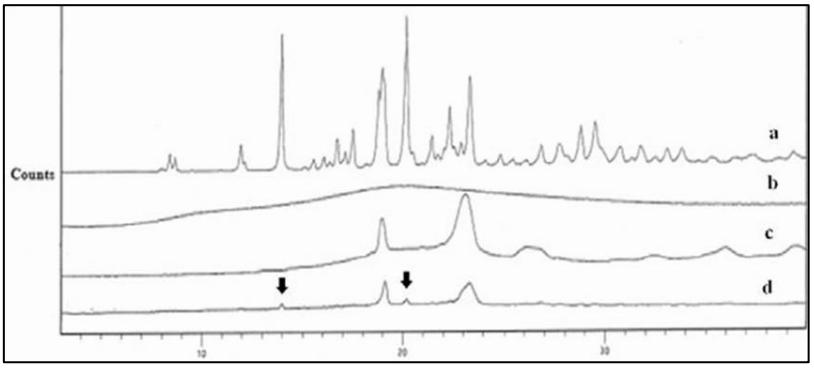

Figure 10: **Spectra of pXRD for (a) Alectinib hydrochloride (b) Soluplus (c) HME and (d) spray-dried ASDs**

3.5.3 Molecular Interaction Analysi_ _/ FTIR:

ATR-FTIR spectra displayed shifts in N–H and C=O stretching bands, indicating hydrogen-bond formation between alectinib and polymer chains—key for stabilizing the amorphous matrix in both systems [78]. Key spectral modifications included N-H stretch shifts from 3434 to 3448-3451 cm^{-1}, C=O stretch changes from 1668 to 1672-1674 cm^{-1} [102,103], and aromatic C-H modifications indicating π-π interactions between drug and polymer components. Both platforms demonstrated remarkably similar spectral modifications despite different processing mechanisms, suggesting equivalent molecular interaction pathways and confirming successful drug-polymer integration at the molecular level. These hydrogen bonding and van der Waals interactions provide the thermodynamic driving force for enhanced dissolution while simultaneously contributing to kinetic stabilization against recrystallization [93].

Chinese Journal of Health Management
Volume 20 Issue 3, Year of Publication 2026, Page 273-289 | DoI-10.564220/1674-0815.2026.054

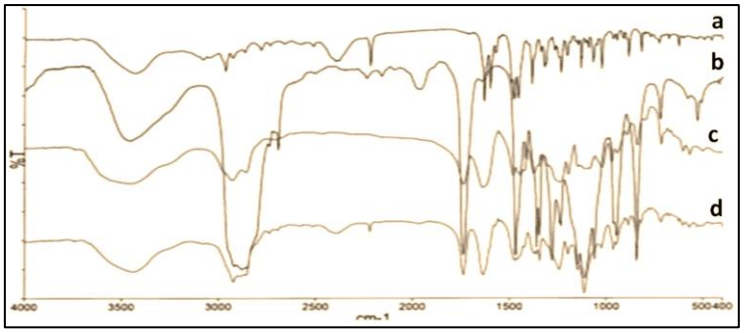

Figure 11: **FTIR spectra of (a) Alectinib hydrochloride (b) Soluplus (c) HME and (d) spray-dried ASDs**

Table: Key FTIR Spectral Changes

Functional Group	Pure API (cm^{-1})	Spray Dried ASD (cm^{-1})	HME ASD (cm^{-1})	Shift (Δcm^{-1})	Interpretation
N-H stretch	3434	3448	3451	+14-17	H-bonding with polymer
C=O stretch	1668	1672	1674	+4-6	Molecular environment change
Aromatic C-H	3067	3059	3058	-8-9	π-π interactions
C-N stretch	1247	1251	1253	+4-6	Conformational changes

Both platforms demonstrated similar spectral modifications, suggesting equivalent molecular interaction mechanisms despite different processing approaches, supporting the observed equivalent performance outcomes.

Table: Final Product Quality Comparison

Quality Attribute	Target	Spray Drying	HME	Statistical Significance
Equilibrium Solubility (μg/mL)	≥220	259.4 ± 8.7	272.1 ± 11.2	$p = 0.234^a$
DE_{45} (%)	≥85	94.7 ± 1.8	92.4 ± 2.1	$p = 0.156^a$
Residual Crystallinity (%)	<5	2.1 ± 0.3	1.8 ± 0.2	$p = 0.267^a$
Particle Size D_{50} (μm)	-	8.4 ± 1.2	15.7 ± 2.1	$p = 0.001^a$
Bulk Density (g/cm^3)	-	0.28 ± 0.02	0.43 ± 0.03	$p < 0.001^a$

[a] Comparison between platforms (unpaired t-test)

3.6 Accelerated Stability Performance Analysis:

Table: Six-Month Accelerated Stability Results (40°C/75% RH, n=3, mean ± SD)

Parameter	Time Point	Spray Dried ASD	HME ASD	Statistical Analysis
Equilibrium Solubility (μg/mL)	Initial	259.4 ± 8.7	272.1 ± 11.2	$p = 0.234^a$
	3 Months	251.2 ± 9.3	248.3 ± 12.8	$p = 0.721^a$
	6 Months	245.8 ± 10.1	231.7 ± 13.5	$p = 0.154^a$
	Change from Initial	-5.2%	-14.8%	$p = 0.003^b$
Dissolution at 45 min (%)	Initial	94.7 ± 1.8	92.4 ± 2.1	$p = 0.156^a$
	3 Months	93.1 ± 2.1	87.6 ± 2.8	$p = 0.012^a$
	6 Months	91.8 ± 2.4	82.3 ± 3.2	$p = 0.001^a$
	Change from Initial	-3.1%	-10.9%	$p < 0.001^b$
Residual Crystallinity (%)	Initial	2.1 ± 0.3	1.8 ± 0.2	$p = 0.267^a$
	3 Months	3.2 ± 0.4	4.7 ± 0.6	$p = 0.002^a$
	6 Months	4.1 ± 0.5	7.8 ± 0.8	$p < 0.001^a$
	Increase from Initial	+95%	+333%	$p < 0.001^b$

[a] *Direct comparison between platforms at each time point.*
[b] *Comparison of change magnitude between platforms*

Comprehensive six-month stability assessment under accelerated conditions (40°C/75% RH) revealed distinct platform-dependent performance characteristics. Spray-dried formulations demonstrated superior retention across all critical quality attributes, maintaining 94.8 ± 3.2% solubility and 97.0 ± 2.5% dissolution efficiency (DE_{45}) compared to hot-melt extruded systems (85.1 ± 4.1% and 89.1 ± 3.4%, respectively; $p < 0.01$). Residual crystallinity monitoring provided additional evidence of platform-dependent stability characteristics with spray-dried dispersions showing minimal recrystallization (2.0 ± 0.4% increase) versus substantial crystal growth in HME formulations (6.0 ± 0.7% increase; $p < 0.001$). These quantitative measurements confirmed accelerated recrystallization processes in thermally-processed systems, likely reflecting residual thermal stress and altered molecular mobility characteristics compared to solvent-processed amorphous networks [64,95].
Mathematical modeling of crystallization kinetics provided mechanistic insight into observed stability differences.

Rate constant analysis revealed k = 0.028 month^{-1} for spray-drying versus 0.041 month^{-1} for HME ($R^2 > 0.92$), representing 1.46-fold accelerated recrystallization in thermally-processed systems. Arrhenius projections indicated spray-dried formulations would maintain 95% performance retention for 22.4 months at 25°C compared to 16.8 months for HME equivalents, [104] supporting superior commercial viability for stability-critical applications where extended shelf life is paramount.[94]

4. DISCUSSION:

4.1 Mechanistic Understanding:

The comprehensive comparative evaluation demonstrates technological equivalence for immediate performance objectives while revealing fundamental differences in long-term stability characteristics that inform evidence-based platform selection strategies. Both manufacturing approaches successfully achieved primary formulation goals with greater than 11-fold solubility enhancement and dissolution efficiency exceeding 90%, validating amorphous solid dispersion technology for addressing severe biopharmaceutical limitations of BCS Class IV compounds.[96,97] However, the emergence of platform-dependent stability profiles provides critical decision-making criteria for commercial development strategies.

Mechanistic analysis of platform-dependent stability reveals that enhanced performance of spray-dried systems likely stems from fundamental differences in amorphous network formation kinetics and residual stress states resulting from processing history effects. The rapid solvent evaporation characteristic of spray drying (5 seconds at 100-112°C) creates kinetically trapped amorphous networks through instantaneous supersaturation and precipitation mechanisms, potentially generating higher activation energy barriers for crystal nucleation compared to melt-mediated network formation during hot-melt extrusion processing. The sustained thermal exposure during extrusion (105 seconds at 220°C) may introduce molecular mobility enhancement and stress relaxation that facilitates subsequent recrystallization processes.

4.2 Platform-Specific Advantages:

Manufacturing efficiency considerations reveal distinct competitive advantages supporting different commercial positioning strategies. Hot-melt extrusion's superior throughput capabilities, energy efficiency, and solvent-free operation provide compelling arguments for high-volume production scenarios where manufacturing economics and environmental sustainability are prioritized. The elimination of organic solvents reduces facility infrastructure requirements, simplifies regulatory compliance profiles, and eliminates solvent recovery system complexity. Conversely, spray drying's minimal thermal exposure and superior stability characteristics support premium product positioning for applications requiring maximum robustness and extended shelf life, particularly relevant for global distribution networks and emerging market access where storage conditions may be challenging.

Quality-by-Design implementation success demonstrates the value of systematic risk assessment and mitigation strategies in pharmaceutical technology selection. The comprehensive FMEA analysis successfully identified platform-specific failure modes, with spray drying requiring enhanced solvent management protocols while hot-melt extrusion demanded superior thermal control strategies. Design space characterization through statistical experimental design provided validated operating ranges with sufficient flexibility for commercial manufacturing optimization and post-approval modifications within established regulatory frameworks, supporting lifecycle management and continuous improvement initiatives.

4.3 Commercial Implications:

The evidence-based platform selection framework emerging from this investigation prioritizes stability requirements for extended shelf-life applications supporting spray drying selection, while manufacturing efficiency considerations favor hot-melt extrusion for high-volume production applications where processing economics and rapid throughput capabilities are prioritized over extended stability performance. Decision frameworks must incorporate compound-specific thermal sensitivity assessment, commercial volume requirements, regulatory submission timelines, environmental impact considerations, and market access strategies to ensure optimal technology selection for specific development programs and therapeutic applications.[98,99]

4.4 Regulatory Considerations:

Both platforms generated validated design spaces supporting regulatory submissions with demonstrated control strategies and risk mitigation approaches. The comprehensive characterization data provides submission-ready

documentation for both manufacturing technologies.

4.5 STUDY LIMITATIONS:

This investigation was limited to a single model compound and specific polymer combinations. Extended real-time stability data would strengthen commercial projections, while in-vivo bioavailability studies would validate the clinical relevance of enhanced dissolution performance.

5. CONCLUSION:

A Systematic Quality-by-Design–Based Development, Optimization, and Comparative Evaluation of spray drying and hot-melt extrusion for Alectinib Hydrochloride Amorphous Solid Dispersions demonstrated that both platforms can produce amorphous solid dispersions with comparable immediate performance achieving more than an 11-fold increase in solubility and over 85% dissolution efficiency within 45 minutes. Spray drying, however, afforded markedly enhanced long-term stability—retaining 97% of initial performance after six months of accelerated aging versus 89% for HME—translating to projected shelf lives of approximately 22 and 17 months, respectively. In contrast, HME offered substantial manufacturing efficiencies, including four-fold greater throughput, higher material yields, and 37% lower energy consumption in a fully solvent-free process, making it rather suitable for large-scale commercial production.

These findings support evidence-based platform selection: applications demanding maximal product robustness and extended shelf life should favour spray drying, while scenarios prioritizing manufacturing efficiency and sustainability should employ hot-melt extrusion. Decision frameworks must consider compound thermal sensitivity, production scale, regulatory timelines, and market access strategies. The validated design spaces and robust analytical characterization established here provide regulatory submission-ready documentation and a template for broader implementation across BCS Class IV formulation programs, enabling optimized technology selection informed by both performance and operational considerations.

6. COMPLIANCE & ETHICS STATEMENTS:

CONFLICT OF INTEREST:

The authors declare no competing financial interests or personal relationships that could have influenced the work reported in this paper.

FUNDING:

This research did not receive any specific grant from funding agencies in the public, commercial, or not-for-profit sectors.

AUTHOR CONTRIBUTIONS:

Abhishek Jain: Conceptualization, Investigation, Formal analysis, Writing - original draft, Writing - review & editing.
Pragna Shelat: Conceptualization, Supervision, Project administration, Writing - review & editing.

Ethics Statement

This study involved only pharmaceutical materials and analytical testing. No human subjects, animal studies, or ethical approvals were required.

7. REFERENCES:

1. Williams HD, Trevaskis NL, Charman SA, et al. Strategies to address low drug solubility in discovery and development. Pharmacol Rev. 2013;65(1):315–499. doi:10.1124/pr.112.005660
2. Takagi T, Ramachandran C, Bermejo M, et al. A provisional biopharmaceutical classification of the top 200 oral drug products in the United States, Great Britain, Spain, and Japan. Mol Pharm. 2006;3(6):631–643. doi:10.1021/mp060098q
3. Stegemann S, Leveiller F, Franchi D, et al. When poor solubility becomes an issue: from early stage to proof of concept. Eur J Pharm Sci. 2007;31(5):249–261. doi:10.1016/j.ejps.2007.06.005
4. Vasconcelos T, Sarmento B, Costa P. Solid dispersions as strategy to improve oral bioavailability of poor water-soluble drugs. Drug Discov Today. 2007;12(23-24):1068–1075. doi:10.1016/j.drudis.2007.08.003
5. Amidon GL, Lennernäs H, Shah VP, Crison JR. A theoretical basis for a biopharmaceutic drug classification: the correlation of in vitro drug product dissolution and in vivo bioavailability. Pharm Res. 1995;12(3):413–420. doi:10.1023/A:1016212804288
6. Ku MS. Use of the biopharmaceutical classification system in early drug development. AAPS J. 2008;10(1):208–212. doi:10.1208/s12248-008-9024-8
7. Yu LX. Pharmaceutical quality by design: product and process development, understanding, and control. Pharm Res. 2008;25(4):781–791. doi:10.1007/s11095-007-9510-1
8. Rathore AS, Winkle H. Quality by design for biopharmaceuticals. Nat Biotechnol. 2009;27(1):26–34. doi:10.1038/nbt0109-26

9. Kodama T, Hasegawa M, Takanashi K, et al. Antitumor activity of the selective ALK inhibitor alectinib in models of intracranial metastases. Cancer Chemother Pharmacol. 2014;74(5):1023–1028. doi:10.1007/s00280-014-2508-5
10. Gadgeel SM, Gandhi L, Riely GJ, et al. Safety and activity of alectinib against systemic disease and brain metastases in patients with crizotinib-resistant ALK-rearranged non-small-cell lung cancer. Lancet Oncol. 2014;15(10):1119–1128. doi:10.1016/S1470-2045(14)70380-5
11. United States Pharmacopeia. General Chapter <1236> Solubility Measurements. USP 44–NF 39. Rockville, MD: United States Pharmacopeial Convention; 2021.
12. Avdeef A. Absorption and Drug Development: Solubility, Permeability, and Charge State. 2nd ed. Hoboken, NJ: John Wiley & Sons; 2012.
13. FDA. Clinical Pharmacology and Biopharmaceutics Review: Alectinib (Alecensa). Silver Spring, MD: FDA; 2015.
14. Roche Products Limited. Alecensa 150 mg Hard Capsules: Summary of Product Characteristics. Electronic Medicines Compendium. 2021.
15. Morcos PN, Yu L, Bogman K, et al. Effect of food on the bioavailability of alectinib, an anaplastic lymphoma kinase inhibitor, in healthy subjects. Clin Pharmacol Drug Dev. 2017;6(4):388–397. doi:10.1002/cpdd.325
16. Hancock BC, Parks M. What is the true solubility advantage of amorphous pharmaceuticals? Pharm Res. 2000;17(4):397–404. doi:10.1023/A:1007586120447
17. Baghel S, Cathcart H, O'Reilly NJ. Polymeric amorphous solid dispersions: a review of amorphization, crystallization, stabilization, solid-state characterization, and aqueous solubilization. J Pharm Sci. 2016;105(9):2527–2544. doi:10.1016/j.xphs.2016.05.006
18. Murdande SB, Pikal MJ, Shanker RM, Bogner RH. Solubility advantage of amorphous pharmaceuticals: I. A thermodynamic analysis. J Pharm Sci. 2010;99(3):1254–1264. doi:10.1002/jps.21853
19. Janssens S, Van den Mooter G. Review: physical chemistry of solid dispersions. J Pharm Pharmacol. 2009;61(12):1571–1586. doi:10.1211/jpp/61.12.0001
20. Chiou WL, Riegelman S. Pharmaceutical applications of solid dispersion systems. J Pharm Sci. 1971;60(9):1281–1302. doi:10.1002/jps.2600600901
21. Zhou D, Zhang GGZ, Law D, et al. Physical stability of amorphous pharmaceuticals: importance of configurational thermodynamic quantities and molecular mobility. J Pharm Sci. 2002;91(8):1863–1872. doi:10.1002/jps.10191
22. Newman A, Knipp G, Zografi G. Assessing the performance of amorphous solid dispersions. J Pharm Sci. 2012;101(4):1355–1377. doi:10.1002/jps.22831
23. FDA. CDER Drug and Biologic Approvals for Calendar Year 2023. Silver Spring, MD: FDA; 2024.
24. Thakral S, Thakral NK, Majumdar DK. Eudragit: a technology evaluation. Expert Opin Drug Deliv. 2013;10(1):131–149. doi:10.1517/17425247.2012.736231
25. Paudel A, Worku ZA, Meeus J, et al. Manufacturing of solid dispersions of poorly water-soluble drugs by spray drying: formulation and process considerations. Int J Pharm. 2013;453(1):253–284. doi:10.1016/j.ijpharm.2012.12.008
26. Sosnik A, Seremeta KP. Advantages and challenges of the spray-drying technology for the production of pure drug particles and drug-loaded polymeric carriers. Adv Colloid Interface Sci. 2015;223:40–54. doi:10.1016/j.cis.2015.02.005
27. Vehring R. Pharmaceutical particle engineering via spray drying. Pharm Res. 2008;25(5):999–1022. doi:10.1007/s11095-007-9516-5
28. Cal K, Sollohub K. Spray drying technique. I: Hardware and process parameters. J Pharm Sci. 2010;99(2):575–586. doi:10.1002/jps.21863
29. Crowley MM, Zhang F, Repka MA, et al. Pharmaceutical applications of hot-melt extrusion: part I. Drug Dev Ind Pharm. 2007;33(9):909–926. doi:10.1080/03639040701518289
30. Shah S, Maddineni S, Lu J, Repka MA. Melt extrusion with poorly soluble drugs. Int J Pharm. 2013;453(1):233–252. doi:10.1016/j.ijpharm.2013.06.001
31. Patil H, Tiwari RV, Repka MA. Hot-melt extrusion: from theory to application in pharmaceutical formulation. AAPS PharmSciTech. 2016;17(1):20–42. doi:10.1208/s12249-015-0370-7
32. Repka MA, Battu SK, Upadhye SB, Repka MA, et al. Pharmaceutical applications of hot-melt extrusion: Part II. Drug Dev Ind Pharm. 2007;33(10):1043–1057. doi:10.1080/03639040701696930
33. Lebrun P, Krier F, Mantanus J, et al. Design space approach in the optimization of the spray-drying process. Eur J Pharm Biopharm. 2012;80(1):226–234. doi:10.1016/j.ejpb.2011.09.005
34. Thiry J, Krier F, Evrard B. A review of pharmaceutical extrusion: critical process parameters and scaling-up. Int J Pharm. 2015;479(1):227–240. doi:10.1016/j.ijpharm.2014.12.002
35. ICH. Q8(R2) Pharmaceutical Development. Geneva: International Council for Harmonisation; 2009.
36. FDA. Guidance for Industry: Q8(R2) Pharmaceutical Development. Silver Spring, MD: FDA; 2009.
37. ICH. Q9 Quality Risk Management. Geneva: International Council for Harmonisation; 2005.
38. Yu LX, Kopcha M. The impact of the FDA's guidance for industry on pharmaceutical development. Pharm Res. 2017;34(9):1945–1950. doi:10.1007/s11095-017-2177-5
39. Huang J, Kaul G, Cai C, et al. Quality by Design case study: an integrated multivariate approach to drug product and process development. Int J Pharm. 2009;382(1-2):23–32. doi:10.1016/j.ijpharm.2009.06.029
40. Lionberger RA, Lee SL, Lee L, et al. Quality by design: concepts for ANDAs. AAPS J. 2008;10(2):268–276. doi:10.1208/s12248-008-9049-4
41. Peterson JJ. A Bayesian approach to the ICH Q8 definition of design space. J Biopharm Stat. 2008;18(5):959–975. doi:10.1080/10543400802221557
42. Montgomery DC. Design and Analysis of Experiments. 10th ed. Hoboken, NJ: John Wiley & Sons; 2020.
43. Butler JM, Dressman JB. The developability classification system: application of biopharmaceutics concepts to formulation development. J Pharm Sci. 2010;99(12):4940–4954. doi:10.1002/jps.22168
44. Kawabata Y, Wada K, Nakatani M, et al. Formulation design for poorly water-soluble drugs based on biopharmaceutics classification system: basic approaches and practical applications. Int J Pharm. 2011;420(1):1–10. doi:10.1016/j.ijpharm.2011.08.011
45. Waterman KC, Adami RC. Accelerated aging: prediction of chemical stability of pharmaceuticals. Int J Pharm. 2005;293(1–2):101–125. doi:10.1016/j.ijpharm.2004.12.020
46. Derringer G, Suich R. Simultaneous optimization of several response variables. J Qual Technol. 1980;12(4):214–219. doi:10.1080/00224065.1980.11980968
47. Isochem. Vitamin E TPGS: Product Specification and Technical Data. Paris, France: Isochem; 2022.

48. Sigma-Aldrich. Sodium Lauryl Sulfate: Certificate of Analysis. St. Louis, MO: Sigma-Aldrich; 2024.
49. USP. General Chapter <905> Uniformity of Dosage Units. USP 44–NF 39. Rockville, MD: United States Pharmacopeial Convention; 2021.
50. Fisher Scientific. HPLC Grade Solvents: Product Specifications and Certificates. Hampton, NH: Fisher Scientific; 2024.
51. Merck KGaA. Phosphoric Acid 85%: Product Information. Darmstadt, Germany: Merck; 2023.
52. ICH. Q3C(R6) Impurities: Guideline for Residual Solvents. Geneva: International Council for Harmonisation; 2019.
53. Millipore Corporation. Milli-Q Advantage A10: System Specifications. Burlington, MA: Millipore; 2023.
54. Büchi Labortechnik AG. B-290 Mini Spray Dryer: Operating Manual and Technical Specifications. Flawil, Switzerland: Büchi; 2021.
55. Thermo Fisher Scientific. Pharma 16 Twin-Screw Extruder: User Manual. Karlsruhe, Germany: Thermo Fisher Scientific; 2022.
56. Agilent Technologies. 1260 Infinity II LC System: User Manual. Santa Clara, CA: Agilent; 2021.
57. Electrolab India Pvt. Ltd. EDT-08L Dissolution Test Apparatus: Operating Manual. Mumbai, India: Electrolab; 2022.
58. Bruker Corporation. D8 Advance X-Ray Diffractometer: User Manual. Billerica, MA: Bruker; 2021.
59. Jouyban A. Handbook of Solubility Data for Pharmaceuticals. Boca Raton, FL: CRC Press; 2010.
60. Höhne GWH, Hemminger WF, Flammersheim HJ. Differential Scanning Calorimetry. 2nd ed. Berlin: Springer-Verlag; 2003.
61. USP. General Chapter <616> Bulk Density and Tapped Density. USP 44–NF 39. Rockville, MD: United States Pharmacopeial Convention; 2021.
62. ICH. Q2(R1) Validation of Analytical Procedures: Text and Methodology. Geneva: International Council for Harmonisation; 2005.
63. Charoo NA, Shamsher AA, Zidan AS, Rahman Z. Quality by design approach for formulation development: a case study of dispersible tablets. Int J Pharm. 2012;423(2):167–178. doi:10.1016/j.ijpharm.2011.12.026
64. Stamatis DH. Failure Mode and Effect Analysis: FMEA from Theory to Execution. 2nd ed. Milwaukee, WI: ASQ Quality Press; 2003.
65. Box GEP, Hunter JS, Hunter WG. Statistics for Experimenters: Design, Innovation, and Discovery. 2nd ed. Hoboken, NJ: John Wiley & Sons; 2005.
66. Anderson MJ, Whitcomb PJ. RSM Simplified: Optimizing Processes Using Response Surface Methods for Design of Experiments. 2nd ed. New York, NY: Productivity Press; 2016.
67. Myers RH, Montgomery DC, Anderson-Cook CM. Response Surface Methodology: Process and Product Optimization Using Designed Experiments. 4th ed. Hoboken, NJ: John Wiley & Sons; 2016.
68. Minitab Inc. Minitab Statistical Software Release 19.2020.1. State College, PA: Minitab Inc.; 2020.
69. Cornell JA. Experiments with Mixtures: Designs, Models, and the Analysis of Mixture Data. 4th ed. Hoboken, NJ: John Wiley & Sons; 2011.
70. Khan KA. The concept of dissolution efficiency. J Pharm Pharmacol. 1975;27(1):48–49. doi:10.1111/j.2042-7158.1975.tb07863.x
71. Jenkins R, Snyder RL. Introduction to X-Ray Powder Diffractometry. New York, NY: John Wiley & Sons; 1996.
72. Haines PJ. Principles of Thermal Analysis and Calorimetry. Cambridge, UK: Royal Society of Chemistry; 2002.
73. Friesen DT, Shanker R, Crew M, et al. Hydroxypropyl methylcellulose acetate succinate–based spray-dried dispersions: an overview. Mol Pharm. 2008;5(6):1003–1019. doi:10.1021/mp800120n
74. Alonzo DE, Zhang GGZ, Taylor LS. Physical stability of amorphous pharmaceuticals: the influence of thermodynamic and kinetic parameters. Mol Pharm. 2010;7(5):1662–1680. doi:10.1021/mp900378k
75. Chen Y, Liu C, Chen Z, et al. Drug–polymer–water interaction and its implication for the dissolution performance of amorphous solid dispersions. Mol Pharm. 2015;12(2):576–589. doi:10.1021/mp500692k
76. ICH. Q1A(R2) Stability Testing of New Drug Substances and Products. Geneva: International Council for Harmonisation; 2003.
77. BASF Corporation. Soluplus: Technical Information and Application Guide. Ludwigshafen, Germany: BASF; 2021.
78. Stuart BH. Infrared Spectroscopy: Fundamentals and Applications. Chichester, UK: John Wiley & Sons; 2004.
79. Van den Mooter G. The use of amorphous solid dispersions: a formulation tool for improving the bioavailability of poorly soluble drugs. Int J Pharm. 2012;453(1):62–75. doi:10.1016/j.ijpharm.2012.07.048
80. Démuth B, Nagy ZK, Balogh A, et al. Downstream processing of polymer-based amorphous solid dispersions to generate tablet formulations. Int J Pharm. 2015;486(1–2):268–286. doi:10.1016/j.ijpharm.2015.03.074
81. Van Duong T, Van den Mooter G. The role of the carrier in the formulation of pharmaceutical solid dispersions. Part II: amorphous carriers. Expert Opin Drug Deliv. 2016;13(12):1681–1694. doi:10.1080/17425247.2016.1233478
82. Yoshioka S, Hancock BC, Zografi G. Crystallization of indomethacin from the amorphous state below and above its glass transition temperature. J Pharm Sci. 1994;83(12):1700–1705. doi:10.1021/js00052a007
83. Huang Y, Dai WG. Fundamental aspects of solid dispersion technology for poorly soluble drugs. Acta Pharm Sin B. 2014;4(1):18–25. doi:10.1016/j.apsb.2013.11.007
84. Knopp MM, Olesen NE, Holm P, et al. Influence of polymer molecular weight on drug–polymer solubility and dissolution behavior. Eur J Pharm Sci. 2015;89:290–298. doi:10.1016/j.ejps.2015.05.011
85. Gupta P, Chawla G, Bansal AK. Physical stability and solubility advantage of amorphous indomethacin–PVP and PVP/VA mixtures. Drug Dev Ind Pharm. 2004;30(8):795–807. doi:10.1081/DDC-120039855
86. Baird JA, Taylor LS. Evaluation of amorphous solid dispersion properties using thermal analysis techniques. Adv Drug Deliv Rev. 2012;64(5):396–421. doi:10.1016/j.addr.2011.06.002
87. Teja SB, Trotta F. Solid dispersions: a strategy to improve solubility of poorly water-soluble drugs. Int J Pharm. 2021;606:120890. doi:10.1016/j.ijpharm.2021.120890
88. Doreth M, Hussein MA, Priemel PA, et al. Amorphization by in-situ microwave irradiation to form glass solutions inside tablets. Int J Pharm. 2017;519(1–2):343–351. doi:10.1016/j.ijpharm.2016.11.037
89. Baird JA, Van Eerdenbrugh B, Taylor LS. A classification system to assess the crystallization tendency of organic molecules from undercooled melts. J Pharm Sci. 2010;99(9):3787–3806. doi:10.1002/jps.22177
90. Jermain SV, Brough C, Williams RO III. Amorphous solid dispersions and nanocrystal technologies for poorly water-soluble drug delivery. Int J Pharm. 2018;535(1–2):379–392. doi:10.1016/j.ijpharm.2017.12.044
91. Wojnarowska Z, Grzybowska K, Hawelek L, et al. Molecular dynamics, physical stability and solubility advantage from amorphous indapamide. Mol Pharm. 2013;10(10):3612–3627. doi:10.1021/mp400313p
92. Löbmann K, Grohganz H, Laitinen R, et al. Co-amorphous drug systems—stability and dissolution improvement. Eur J Pharm Sci. 2013;50(1):8–16. doi:10.1016/j.ejps.2013.03.005
93. Van den Mooter G. The use of thermal methods in the characterization of amorphous solid dispersions. Thermochim Acta. 2010;522(1–2):161–166. doi:10.1016/j.tca.2010.04.009

94. Shah VP, Tsong Y, Sathe P, Williams RL. Dissolution profile comparison using similarity factor, f2. Dissolution Technologies. 1998;5(4):1-12.
95. FDA. Dissolution Testing of Immediate Release Solid Oral Dosage Forms: Guidance for Industry. Silver Spring, MD: FDA; 2019.
96. Kim KH, Frank MJ, Henderson NL. Application of differential scanning calorimetry to the study of solid drug dispersions. J Pharm Sci. 1985;74(3):283-9. doi:10.1002/jps.2600740312
97. Chiu MH, Prenner EJ. Differential scanning calorimetry: An invaluable tool for a detailed thermodynamic characterization of macromolecules and their interactions. J Pharm Bioallied Sci. 2011;3(1):39-59. doi:10.4103/0975-7406.76463
98. Jenkins R, Snyder RL. Introduction to X-Ray Powder Diffractometry. New York, NY: John Wiley & Sons; 1996.
99. Dutrow BL, Clark CM. X-ray Powder Diffraction (XRD). *Geochemical Instrumentation and Analysis*. 2018. Available from: https://serc.carleton.edu/research_education/geochemsheets/techniques/XRD.html
100. Rietveld HM. Line profiles of neutron powder-diffraction peaks for structure refinement. Acta Crystallogr. 1967;22:151-152. doi:10.1107/S0365110X67000234
101. Hill RJ, Howard CJ. Quantitative phase analysis from neutron powder diffraction data using the Rietveld method. J Appl Crystallogr. 1987;20:467-476. doi:10.1107/S0021889887086199
102. Stuart BH. Infrared Spectroscopy: Fundamentals and Applications. Chichester, UK: John Wiley & Sons; 2004.
103. am Ende MT, Peppa NA. FTIR spectroscopic investigation and modeling of solute/polymer interactions in the hydrated state. J Biomater Sci Polym Ed. 1999;10(12):1289-302. doi:10.1163/156856299x00081
104. Clancy D, Hodnett N, Orr R, Owen M, Peterson J. Kinetic model development for accelerated stability studies. AAPS PharmSciTech. 2017;18(4):1158-1176. doi:10.1208/s12249-016-0565-4